Oil & Gas Science and Technology – Rev. IFP, Vol. 58 (2003), No. 1, pp. 79-100
Copyright © 2003, Éditions Technip

Use of Advanced Tools for the Analysis of Gasoline Direct Injection Engines

M. Castagné[1], J.P. Dumas[1], S. Henriot[1] and Ph. Pierre[1]

1 Institut français du pétrole, division Techniques d'applications énergétiques, 1 et 4, avenue de Bois-Préau, 92852 Rueil-Malmaison Cedex - France

e-mail: michel.castagne@ifp.fr - j-pierre.dumas@ifp.fr - stephane.henriot@ifp.fr - philippe.pierre@ifp.fr

Résumé — Utilisation d'outils avancés pour l'analyse des moteurs à injection directe d'essence — Une méthodologie utilisant simultanément des calculs tridimensionnels (3D) et des outils expérimentaux avancés a été développée dans le but de caractériser le mélange air/carburant et la combustion des moteurs à injection directe d'essence (IDE) à tous les stades de développement.

Les outils expérimentaux utilisés soulignent la grande variabilité cyclique et montrent que les dispersions de la richesse du mélange à la bougie sont étroitement liées aux fluctuations du démarrage et du développement de la combustion. Malgré ces dispersions, les mesures moyennes sont reproductibles et en bon accord avec les résultats des calculs 3D obtenus avec le code KIVA-MB. L'utilisation conjointe de ces deux types d'outils permet une compréhension très fine des différents concepts de moteurs IDE.

Cette approche a d'abord été appliquée au concept de moteur IDE à jet dévié par la paroi, à travers l'analyse du moteur *Mitsubishi* GDI. Elle a également été utilisée pour analyser le concept de moteur IDE à stratification par le jet. Dans les deux cas, la robustesse du contrôle de la richesse du mélange à la bougie apparaît clairement comme le challenge le plus difficile pour la mise au point des moteurs IDE stratifiés.

Abstract — Use of Advanced Tools for the Analysis of Gasoline Direct Injection Engines *— A methodology that uses simultaneously three dimensional (3D) calculations and advanced experimental tools has been developed in order to characterize air/fuel mixing and combustion of gasoline direct injection (GDI) engines at every stage of development.*

The experimental tools used in this analysis underline the great cycle-to-cycle variability and show that the air/fuel ratio variations at spark plug are closely linked to the fluctuations of combustion starting and development. Despite this variability, average measurements are reproducible and in good agreement with 3D computational results obtained with KIVA-MB code. The common use of both kinds of tools allows getting a very fine understanding of GDI engine concepts.

This approach has been first applied to the analysis of wall-guided direct injection engine concept, through the analysis of Mitsubishi *GDI engine. It has also been used for the analysis of the spray-guided direct injection engine concept. In both cases the robustness of the air/fuel ratio control at spark plug is clearly the greatest challenge for GDI stratified engines.*

INTRODUCTION

The potential of four-stroke gasoline direct injection (GDI) engines to enhance fuel economy, transient response and cold-start hydrocarbon (HC) emissions has led to a worldwide research and development effort [1, 2].

Due to their great complexity, GDI engines require fine analysis tools during the entire development process. Optical engines can only be used at the early stage of development because of their poor cooling and great brittleness. Moreover due to building constraints, their behavior is not fully representative of industrial engines. An other approach, which uses simultaneously 3D calculations and advanced experimental tools, has been developed in order to characterize air-fuel mixing and combustion of GDI engines, even at a late stage of development.

The *Mitsubishi* GDI 1.8 l engine (Japanese version) was first used to validate this methodology. This engine is the first GDI engine to be marketed [3-6]. The combustion chamber concept of this engine is of the wall-guided type, in which a strong reverse tumble motion conveys the fuel impinging the piston bowl to the spark plug. In this pent-roof cylinder head with four valves per cylinder, the tumble is generated by vertical intake ducts and by the shape of the piston. The geometric compression ratio of 12:1 is high. The fuel is injected at 5 MPa pressure by *Mitsubishi* hollow cone swirl injectors.

The methodology has also been applied to the spray-guided concept, which appears more and more to be the ultimate concept for GDI stratified engines. In this concept, spark occurs in the peripheral whirls of injector spray, where gasoline and air form an inflammable mixture. This principle allows using a high level of air and fuel stratification, which is in favor of fuel consumption and NO_x emissions, but requires a very fine and reproducible control of injector spray. We used a single-cylinder *Renault* 0.5 l engine with a pent-roof four valves cylinder head and a 12 MPa *Siemens* hollow cone swirl injector.

1 PROGRAM

Most of the work was performed on the *Mitsubishi* multi-cylinder engine. Experimental investigations were conducted in parallel with a 3D modeling study.

- For experimental part, wide parametric variations about two basic operating points at 2000 rpm break mean equivalent pressure (BMEP) 200 kPa were realized. One of these points was performed in stratified operation at a manifold pressure of 80 kPa (which corresponds roughly to a global air/fuel ratio of 32.5). The other was performed in homogeneous operation with an air/fuel equivalent ratio of 1.
- The 3D-modeling program included parametric variations about the basic operating point in stratified operation. Complete simulations from intake to combustion, taking account fuel injection, were carried out, and a comparison with the experimentally measured air/fuel equivalent ratio at spark plug was made.

The work performed on the *Renault* single-cylinder engine was only experimental. Two operating points were used: 2000 rpm with indicated mean equivalent pressure (IMEP) 380 kPa and 1000 rpm IMEP 180 kPa. As previously, these points were performed in homogeneous operation and in stratified operation. In the first case air/fuel equivalent ratio was 1. In the last case the manifold pressure was 100 kPa (WOT: wide open throttle) and the global air/fuel equivalent ratio were respectively 2.8 for 2000 rpm IMEP 380 kPa and 5.1 for 1000 rpm IMEP 180 kPa.

For both engines the experimental study could be divided in two parts:

- Characterization of the mixture preparation by visualizing the injection and by measurements of fuel concentration at spark plug by means of high-speed flame ionization detection analyzer (FID).
- Characterization of combustion by endoscopy in the combustion chamber and cylinder pressure measurements (with IMEP calculations).

2 DEDICATED INSTRUMENTATION

Pressure sensors were used to characterize combustion on both engines. In addition to standard instrumentation (exhaust gas analysis, intake and exhaust temperatures and pressures), the test bench was equipped with specific instrumentation.

For visualization inside the cylinder, we used on both engines an AVL (acoustic-velocity log) endoscopy system. Based on one image per engine cycle, this system helps to observe the repeatability of injection or combustion at the same angle or their variations with crank angle (with ability to average the images). This system is composed of an endoscope linked to a camera and a light guide linked to light source, placed in two inserts machined on cylinder head. For both engines special attention was paid to be able to see the fuel arrival and ignition events at spark plug.

For the *Mitsubishi* engine, the system was implemented on another cylinder head as FID, but also on cylinder 1. The photograph and the drawing (*Fig. 1*) below shows the instrumented cylinder head of these systems.

If very rich combustion naturally emits a yellow light, a device for seeding intake air with sodium borate was used on *Mitsubishi* engine to make “conventional” pre-mix type combustion more luminous (white light with intensity depending on gas temperature).

For the *Renault* engine, light guide and camera were also on the same side as shown on left drawing on Figure 2. A special machining of piston has been made in order to be sure

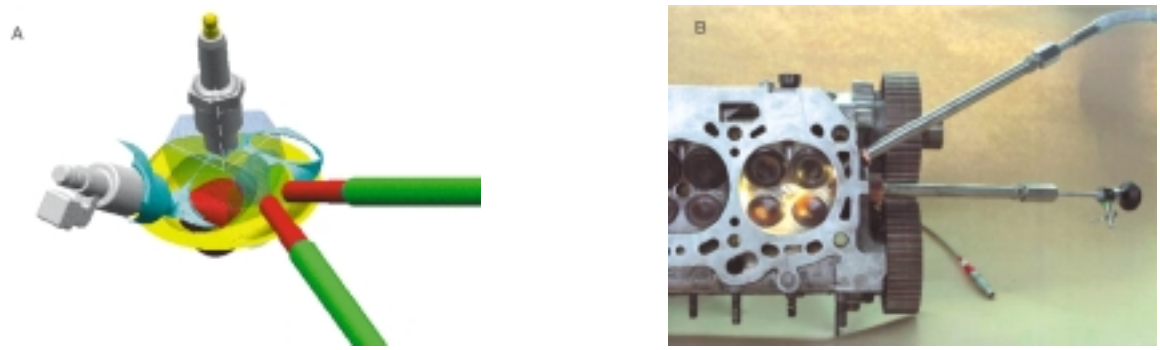

Figure 1

Implementation of endoscopy system on the *Mitsubishi* engine.

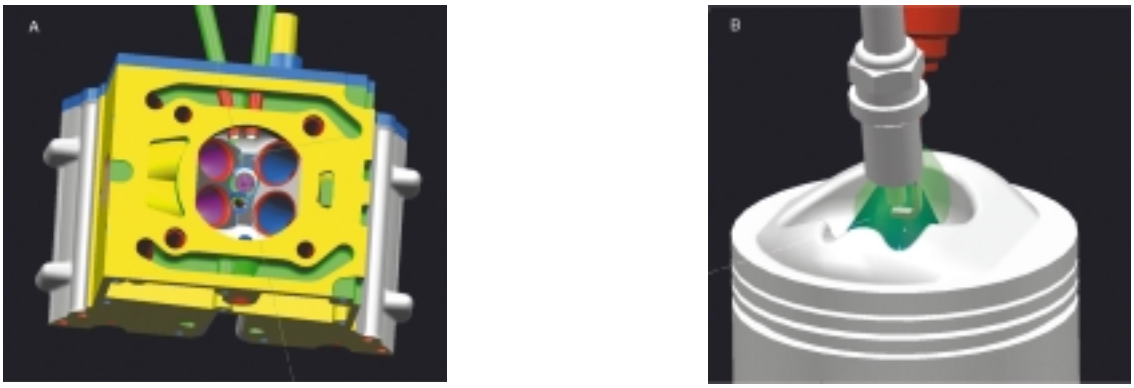

Figure 2

Implementation of endoscopy system on the *Renault* engine.

that the electrodes and the spray could be seen even at top dead center. The right drawing of Figure 2 shows what endoscopy system is able to see.

For measurements of fuel concentration at spark plug, we used an HFR400 fast FID analyzer manufactured by *Cambustion Ltd.* Since this analyzer had two detectors, it was possible to take simultaneous measurements in two locations during the same engine cycles.

We used this opportunity for the analysis of *Mitsubishi* GDI engine. For that, the cylinder head was equipped with two probes placed on the same cylinder than the cooled pressure sensor:

– One probe taking the sample through the spark plug. Sampling was hence carried out along the vertical axis of the engine at a distance of 5 mm from the central electrode of the plug.
– One probe taking the sample through the cylinder head between the exhaust valves at a 45° angle to the vertical axis of the engine. Sampling was carried out on the exhaust valve side at a distance of 4 mm from the plug electrodes.

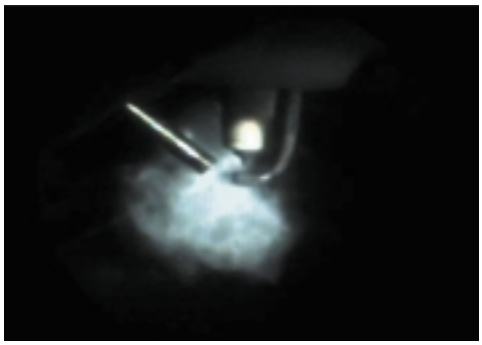

Figure 3

Implementation of FID probe on the *Renault* engine.

To perform tests with a perfectly homogeneous mixture, we supplemented the experimental rig by feeding the engine with propane in the intake.

For *Renault* engine, we used only one probe that was also taking the sample through the cylinder head between the exhaust valves. Special attention was paid to place the probe

as close as possible to the electrode gap without disturbing the spark event and in a good position relative to fuel spray as it can be seen on Figure 3 (image obtained with the endoscopy system).

3 STUDY OF MIXTURE PREPARATION

3.1 Experimental Part

3.1.1 Determination of Fuel Concentration at Spark Plug by High-Speed FID

Principle and Perfecting of the Measurement

The FID analyzer takes a gas sample continuously in the combustion chamber near the spark plug through probes installed on the cylinder head [7, 8]. This sample is then analyzed by the FID technique which delivers a signal proportional to the HC concentration in the sample.

This measurement system demands accurate adjustment of certain components:

– FID burner: the very high concentrations measured (> 100 000 ppm C HC) demands very specific adjustment of the burner to avoid problems of signal saturation (nonlinearity) and synergism (interaction of O_2 present in the sample on the HC measurement). These adjustments required lengthy fine-tuning and had to be monitored constantly throughout the tests.

– Sampling device: the dimensional parameters (probe length and diameter), physical quantities of this device (pressure in the chamber placed upstream of the burner in particular) were adjusted as required to obtain a constant sampling rate in order to have a linear response for subsequent optimization of response time.

Like any measurement of this type, HC measurement by high-speed FID involves a data transfer time and a response time (defined as the time needed to transfer 10 to 90% of the signal during a concentration step).

The transfer time can be discarded by adjusting the timing of the signal by the use of the difference in pressure between the combustion chamber and the constant pressure chamber upstream of the FID burner. While on the contrary, it is not possible to discard the response time, it is nonetheless possible to estimate it by assuming an instantaneous drop in HC concentration on passage of the flame. Figure 4 illustrates the adjustment to be made and the estimation of the response time on a case with propane (perfect mixture homogeneity) at 2000 rpm, BMEP 200 kPa, air/fuel equivalent ratio 1, spark advance 25 CAD (crank angle degree) before top dead center (CAD BTDC) on *Mitsubishi* engine.

As the tests proceeded, optimizing the settings shortened the response time. However, the most important parameter concerning this response time is the length of the probe. For the *Mitsubishi* engine, the probe passing through the plug could not be reduced below 35 cm due to the need to go back through the spark plug well and make a 90° bend to reach the FID head at the horizontal. The optimized response time was about 1.05 ms (12.5 CAD) on this probe. We therefore installed a second probe across the exhaust side, with its length limited to 20 cm. On this probe, the optimized response time was about 0.8 ms (9.5 CAD).

Figure 5 shows the influence of the probe length on the measurement in stratified operation. It was obtained by replacing the 20 cm probe in the same position in the combustion chamber of *Mitsubishi* engine by the 35 cm probe used at the plug on a stratified point with iso-octane.

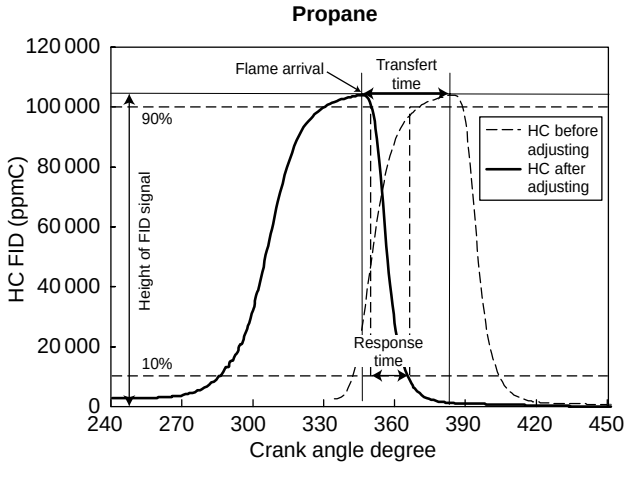

Figure 4

Adjustment of FID signal with propane *(Mitsubishi* engine).

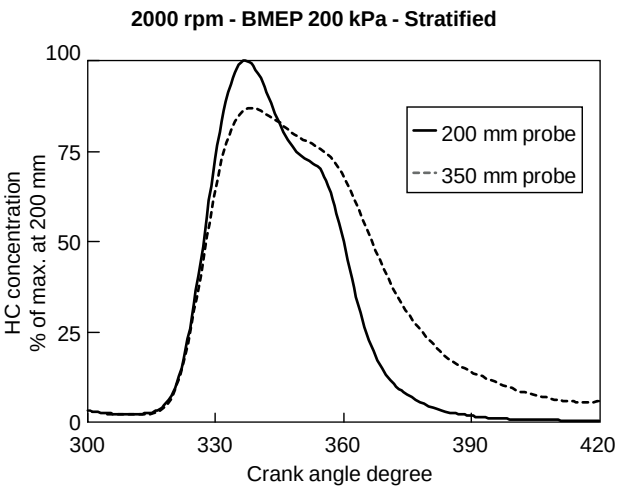

Figure 5

Influence of probe length on FID signal (*Mitsubishi* engine).

Both FID signals are post-processed in order to adjust timing (correction of transfer time only). The effect of signal dilution clearly appears in this comparison.

For the *Renault* engine it was not possible to reduce the length of the probe below 25 cm.

Post-Processing of Results

A software was used to adjust the signal according to the instantaneous cylinder pressure. This program is based on a quasi-steady state one dimensional flow model as Summers, Collings *et al.* [9, 10]. The basis is an isothermal expression for the speed of the flow along the sampling tube of the probe. Because of the variable inlet pressure, a numerical solution is used. As it can be seen in the results, it is the compression and power strokes part of the signal that was computed. Under these conditions, the isothermal flow assumption becomes invalid but Peckham [11] indicated that the maximum error in mass flow evaluation is in this case about 1.5%. The other delays due to FID detector were integrated in the computation. Experimental set-up was adjusted to avoid choking flow during sampling.

This program was validated by comparing the passage of combustion on the FID signal to the signal of the burnt fraction obtained from the pressure signal by combustion analysis. This validation on *Mitsubishi* engine is shown 0n Figure 6.

We also examined the ability to translate the FID signal into local air/fuel equivalent ratio. The problem comes from the fact that the local air/fuel equivalent ratio is also related to the local O_2 content, which is not precisely known in the presence of EGR (exhaust-gas recirculation) or residual gases (their quantity, position and O_2 content must be taken into account).

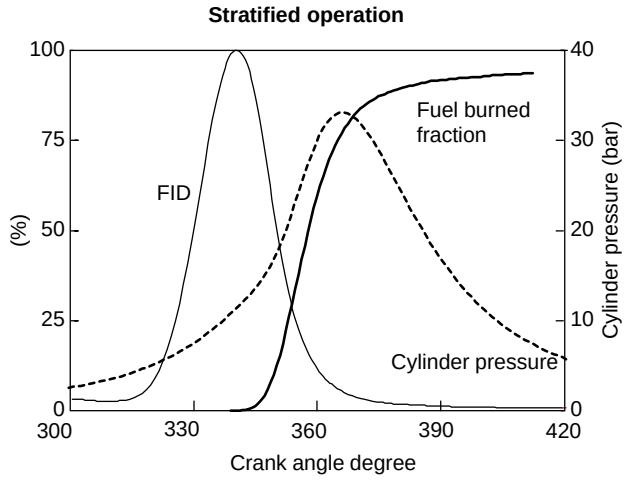

Figure 6

Validation of FID adjustment in stratified mode (*Mitsubishi* engine).

Hence it does not appear feasible to genuinely obtain the local air/fuel equivalent ratio from the FID signal, particularly in stratified operation. Because of this, the comparisons with the 3D calculation presented below are made for HC concentration.

For each case in stratified mode, the HC concentration is expressed relatively to the maximum FID value on a reference setting.

Test Methodology

Methodology for Wall Guided GDI Engines

The first problem that arose concerned the repeatability of the results and the cyclic variations.

In fact, while the FID signal obtained in homogeneous operation, and especially with propane, is relatively repeatable from cycle to cycle, wide cyclic fluctuations were observed in stratified operation. The following comparison was made between the homogeneous and stratified points with the basic settings. On each of these points, we recorded the signals of 250 engine cycles. Figure 7 shows the variations in the maximum FID level reached according to the operating mode and the fuel used.

Figure 8 illustrates the cyclic fluctuations in FID signals (before timing adjustment) for homogeneous and stratified modes. Mean values are in bold.

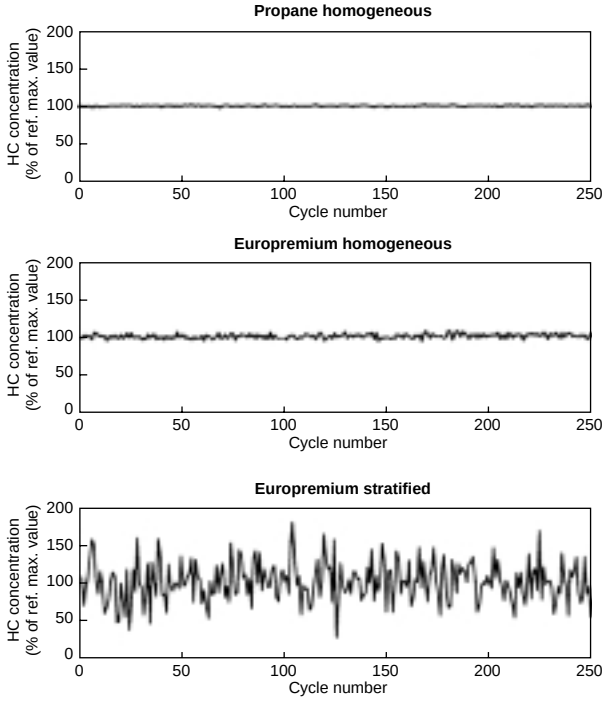

Figure 7

Cycle variations in height of FID signal.

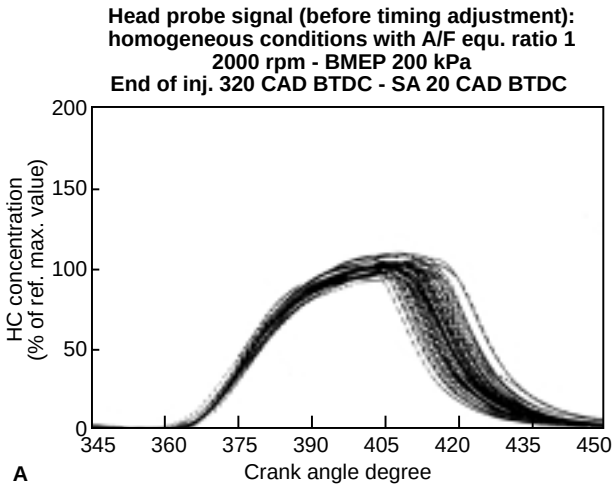

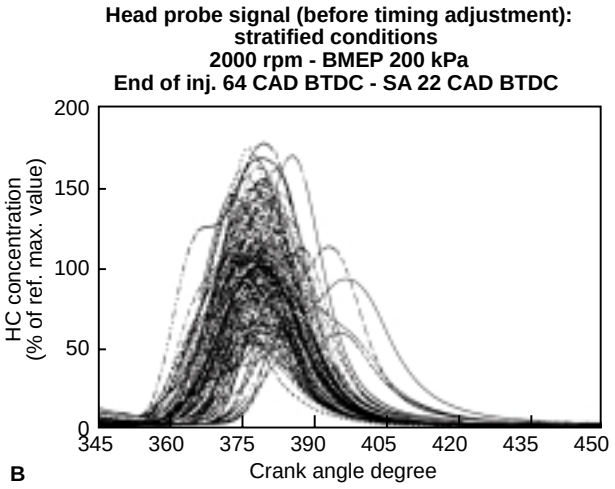

Figure 8

Cycle resolved FID measurement in homogeneous and stratified modes.

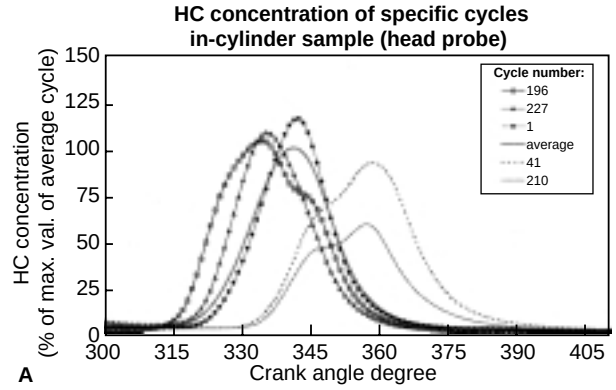

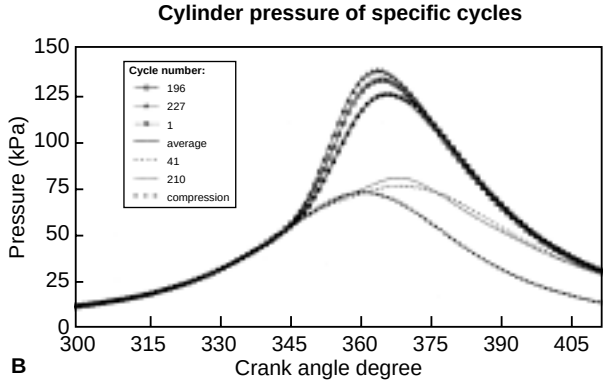

Cycle N	IMEP kPa	Max. pres. kPa	Pmax.angle CAD	FIDmax. % max. average	FIDmax. angle CAD	HLC 1/CAD	HLC angle CAD	CA 10% CAD	CA 50% CAD
196	266	3524	364	104	334	0.079	354.0	351.3	364.9
227	269	3660	363	109	335	0.077	354.0	350.5	362.5
1	280	3316	365	116	342	0.056	354.0	352.7	369.8
Average	**259**	**3328**	**366**	**100**	**341**	**0.053**	**355.5**	**352.4**	**368.8**
41	213	2002	368	92	358	0.027	375.7	374.3	418.9
210	197	2118	367	59	357	0.028	375.7	370.4	430.4

Figure 9

Analysis of individuals cycles.

Fairly good repeatability of the FID signal (but not at all as good as with propane) is observed in homogeneous operation. The widest dispersion concerns the drop in the signal, which is directly related to the passage of the flame.

Very wide dispersion appears in stratified operation in the maximum height of the FID signal, but also in the phasing of this maximum and on the start of combustion.

To check the significance of such a disparity in measurement, and to gauge its consequences accurately, we isolated a number of cycles among those presented above, and compared them, after adjustment, with the corresponding pressure signals, on which we carried out combustion analyses.

Figure 9 (and the corresponding table) shows that the FID signals recorded by the cylinder head probe are well correlated with the corresponding pressure signals and combustion analyses:

– The earliest FID signals (cycles 196 and 227) effectively correspond to an earlier start of combustion.
– The latest FID signals (cycles 41 and 210) correspond to latest start of combustion. While these cycles display IMEP far below the mean, these IMEP are nonetheless very distant from the IMEP that would be displayed by a cycle without combustion.
– A cycle close to the average in terms of FID (cycle 1) logically corresponds (due to the presence of the later or earlier cycles) to a slightly less spread pressure curve, at a slightly higher P_{max} and a higher IMEP.

Cycle 124 corresponds to an interesting case. This cycle in fact displays a normal pressure curve, despite an abnormally low cylinder head FID signal. On further investigation, it appears that the FID signal measured through the spark plug FID probe is rather high, as shown on Figure 10. Hence it

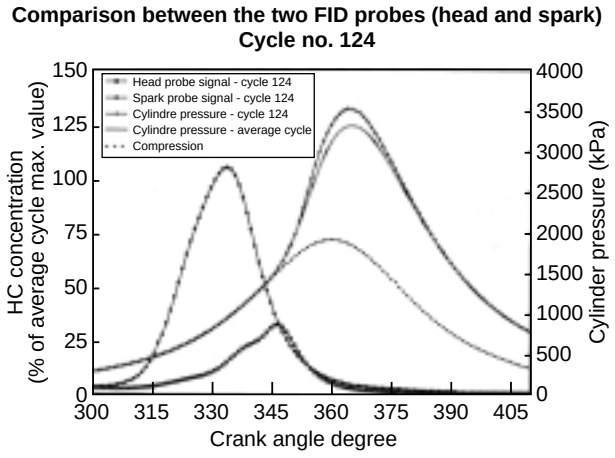

Figure 10

FID specific cycle - Comparison of two probes.

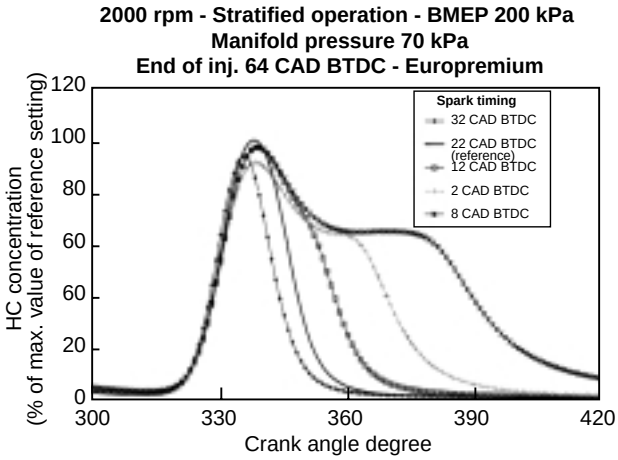

Figure 11

Variation in spark advance about the basic point in stratified mode.

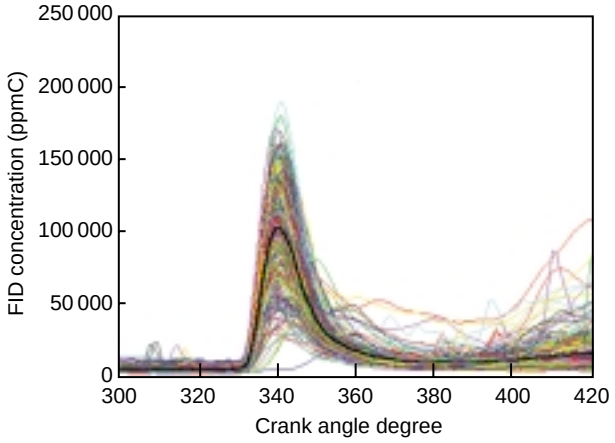

Figure 12

Cycle resolved FID measurement in stratified mode at 1000 rpm - IMEP 180 kPa.

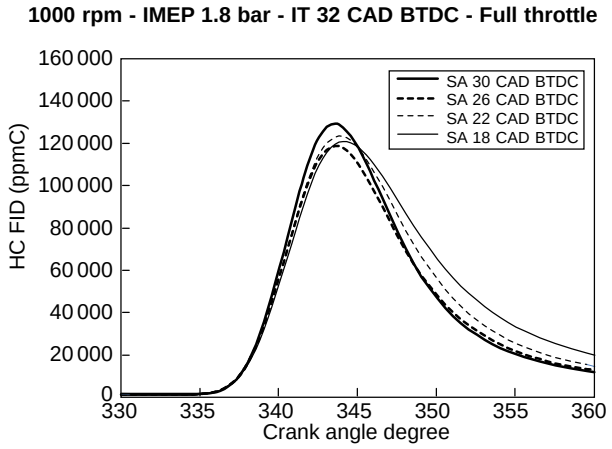

Figure 13

Variation of ignition timing at 1000 rpm - IMEP 180 kPa.

appears that some cycles display considerable stratification of the fuel around the plug, since the two probes are only 7 mm apart.

While the dispersion of the FID measurements clearly seems to reflect the dispersion observed in the progress of combustion and, as such, represents a result of great importance, we nonetheless questioned the significance of the mean signal, as well as its reproducibility.

A specific test methodology was accordingly developed: for each engine operating point, a first measurement was taken with optimal spark advance (SA) followed by four other measurements with shifts in SA. For each of these measurements, we kept the curve corresponding to the mean values between 250 cycles.

Before analyzing the results, it can be noted that despite the wide cycle-to-cycle dispersion, the mean of the adjusted 250 cycles (after individual post-processing) clearly corresponds to the adjustment of the mean of the 250 raw cycles. This can be ascribed to the fact that the flow becomes sonic at the capillary exit, so that the transfer time is not influenced by the pressure above a certain threshold reached during the compression phase.

The usefulness of this procedure is revealed by Figure 11.

This figure clearly shows the reproducibility of the fuel concentration (HC) curve at the spark plug from one spark advance to the next, with a simple time shift at the passage of the flame. This offers a concept of an envelope curve showing that the mean signal clearly qualifies the variation in air/fuel equivalent ratio at the plug on a given operating point and that it accordingly allows point-to-point comparisons. This methodology was systematically applied for all the points of the parametric study.

Methodology For Spray Guided GDI Engines

The repeatability of cycle-to-cycle FID measurements during stratified operations is not better with spray guided engines. Figure 12 shows the cycle-to-cycle and mean HC concentration corresponding to a set point 1000 rpm-IMEP 180 kPa-WOT.

Nevertheless, the repeatability of mean FID measurement over a range of 250 cycles is correct and we tried first to use the same methodology as the one used for wall guided engines. It appears rapidly that the variation in spark advance about the basic point was not useable, because the beginning of combustion event depends less on spark timing than on injection timing with spray guided concept. Figure 13 shows the variation of HC concentration at spark plug according to spark advance on the set point 1000 rpm-IMEP 180 kPa-WOT end injection timing of 32 CAD BTDC.

We develop then an other methodology based on skip firing in order to obtain the envelope curve of HC concentration. This methodology consists in removing the spark event on one cycle out of five and averaging cycles without combustion. It has been preferred to a methodology based on skip injection (one injection over 5 cycles, no firing) because of a better representativeness of combustion chamber parameters (piston temperature, residual gases, etc.). The results with both methodology were nevertheless very closed as shown on Figure 14 obtained with the 1000 rpm-IMEP 180 kPa-WOT set point. These envelope curves are compared with the curve corresponding to the average of firing cycles on the same test. It appears that the maximum heights of FID signal with or without firing are very closed. That validates that combustion initiation occurs after the FID signal begins going down (which is confirmed by heat release calculation) and that FID analyzer response time is suitable for good evaluation of HC concentration at this engine speed.

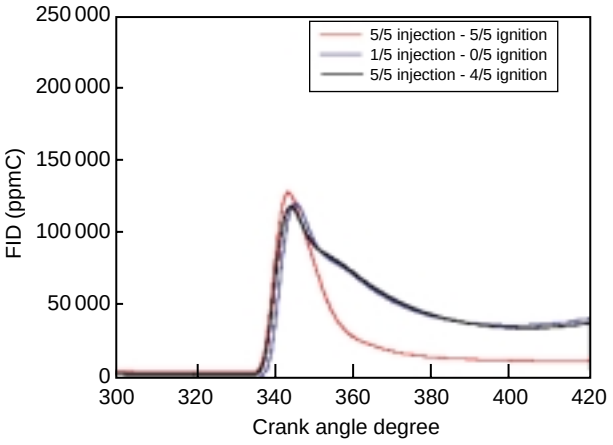

Figure 14

Comparison of skip firing and skip injection methodology at 1000 rpm - IMEP 180 kPa.

With an engine speed of 2000 rpm, the representativeness of FID measurement during spark event on firing cycle is more difficult to assess, because the maximum of FID signal angle is very closed to the beginning of combustion event. In this configuration, it is difficult to be sure that the increase of FID signal during response time is not interrupted by flame and that the value of HC concentration on individual cycles

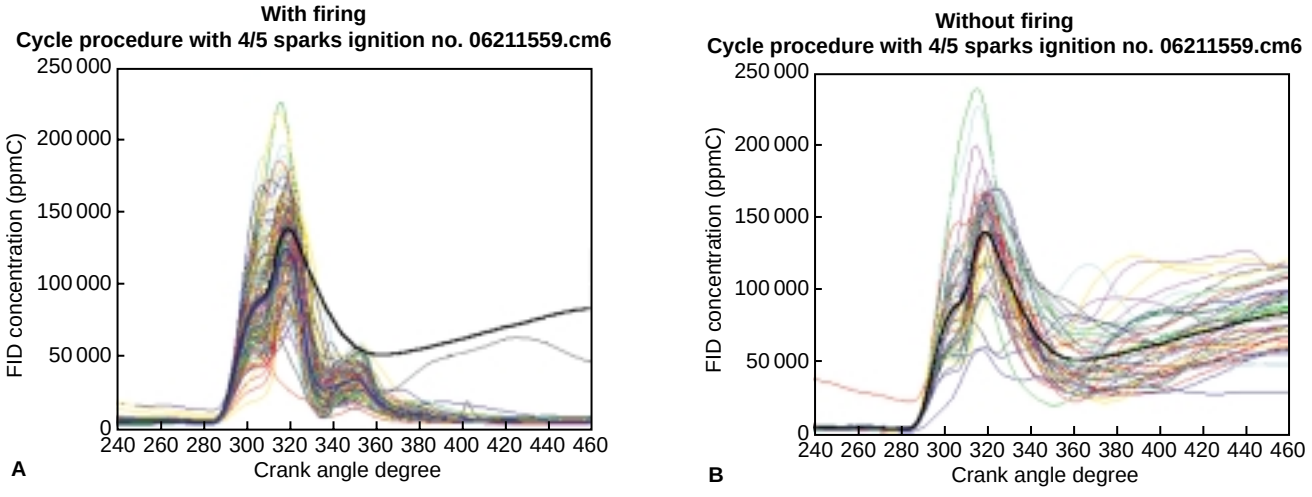

Figure 15

Comparison of cyclic measurement with and without firing 2000 rpm - IMEP 380 kPa - WOT. - End of injection timing 64 CAD BTDC - Spark timing 47 CAD BTDC.

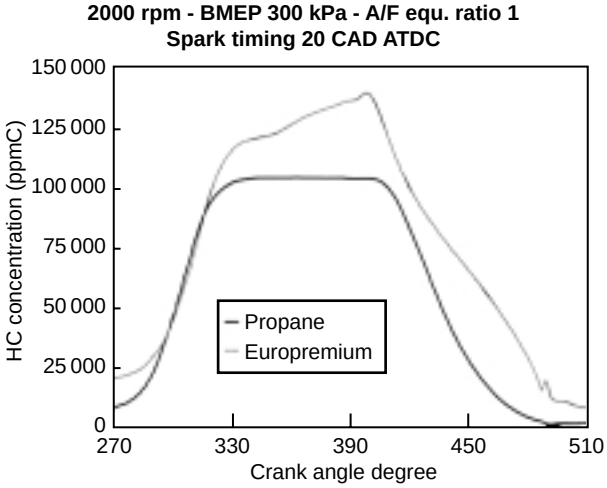

Figure 16

Propane/europremium comparison in homogeneous operation.

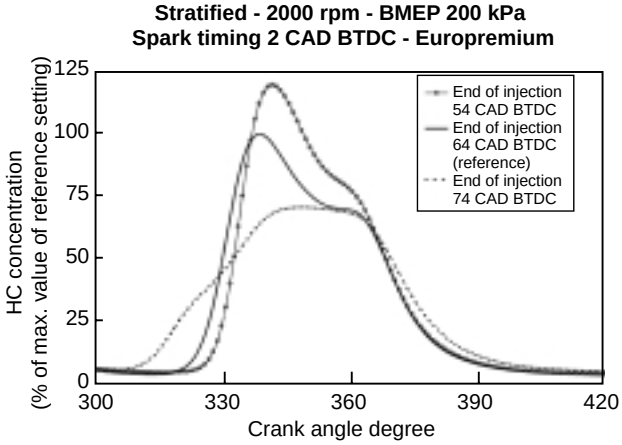

Figure 17

Influence of injection timing in stratified operation.

when firing is not under-estimated. Figure 15 shows the individual cycles with and without firing. Thick black lines represent average values of FID measurement without combustion and thick blue lines with (note that the bump of curve with combustion around 360 CAD is due to flow choking in the FID sampling system).

Cyclic dispersion of fuel concentration at spark plug is very large. Because of the risk that flame interrupts FID signal's rising, curves obtained without firing give a better idea of fuel concentration variations.

Parametric Study

Parametric Study with *Mitsubishi* Wall Guided GDI Concept

- Propane/europremium comparison in homogeneous operation.

The FID signal is found to stabilize at 105 000 ppm C in the case of propane injection upstream of the manifold (*Fig. 16*). We know very accurately the air/fuel equivalent ratio of the mixture introduced in this case (stoechiometry), and can therefore make a rough estimation of the residual gas: knowing that 121 000 ppm C corresponds to a stoechiometric air/propane mixture without residuals, we can estimate the latter at 13% if they are assumed to be uniformly distributed. With europremium, a rise is observed in the signal above air/fuel equivalent ratio 1 (140 000 ppm C without residuals, 122 000 ppm C assuming the same 13% residuals). This is probably related to a fuel deposit on the piston.

- Influence of injection timing in stratified operation.

The injection timing (IT) is expressed by end of injection angle as shown on Figure 17.

It appears that the fuel arrives earlier with the IT of 74 CAD BTDC, but that the FID signal is not as high, indicating greater dilution. Conversely, with the IT of 54 CAD BTDC, the FID signal arrives later but rises much higher, indicating a higher level of stratification. In all three cases, the flame passes at approximately the same angle.

- Influence of load in stratified operation.

A comparison of the tests at different loads raises the problem of the thermodynamic conditions in the cylinder during injection. For set points corresponding to Figure 18, Table 1 can be compiled.

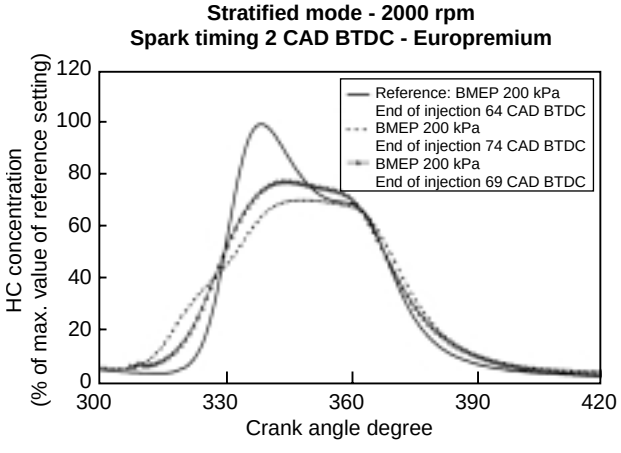

Figure 18

Influence of load in stratified operation.

TABLE 1

Influence of load in stratified operation at 2000 rpm

Set point	1	2	3
BMEP (kPa)	200	200	500
End of injection (CAD BTDC)	64	74	69
Injection duration (ms)	0.850	0.850	1.475
Start of injection (CAD BTDC)	74	84	87
Manifold pressure (kPa)	70	70	100
Cyl. pressure at start of injection (kPa)	191	155	214
Spark advance (CAD BTDC)	2	2	2
Global air/fuel equivalent ratio	2.12	2.12	1.78

If the optimal setting at 200 kPa is the set point 1, the start of injection angle of the optimal setting at 500 kPa is closer to the point 2. Nevertheless, despite a slightly earlier start of injection, the start of the FID signal occurs slightly later at set point 3 than at set point 2. This appears to be due to a higher density of the air, which decreases the penetration of the spray. However, due to the lower air/fuel equivalent ratio, the FID signal rises higher, but not so as for set point 1.

- Influence of engine speed in stratified operation.

On the variation in spark advance at 3000 rpm presented on Figure 19 (which can be compared with the similar test at 2000 rpm discussed earlier), it appears that we have reached the limits of use of FID: it is necessary to await SA 2 CAD BTDC to reach the maximum FID signal, which was previously reached for an SA of 22 CAD BTDC. The effect of signal dilution hence makes this signal difficult to use.

Parametric Study with Spray Guided GDI Concept

- Influence of injection timing in stratified operation.

Mean cycles with and without combustion with different injection timing and same spark advance are presented in Figure 20. The use of skip firing methodology appears necessary, especially for later injection. Fuel arrives earlier with the IT of 64 CAD BTDC, but FID signal is not as high, indicating greater dilution. With the IT of 37 CAD BTDC, FID signal arrives late, rises not high and is relatively constant. The explanation of this behavior is probably that spray cone angle is reduced due to the higher air density and that FID probe is located into the swirls in the border of the spray (see further the visualization of mixture preparation), in a leaner mixture. It must be noted that the FID signal is very sensitive to spay location and shape, which could vary from one test to another according to injector fouling. It is also particularly difficult to ensure the FID probe cleanness and then repeatablity of HC measurement with spray guided concept.

3.1.2 Visualization of Mixture Preparation by Endoscopy

Endoscopy appears to be a useful means for visualizing the route of the fuel in the cylinder.

Visualizations of Mixture Preparation on Mitsubishi *Wall Guided GDI Engine*

The Figure 21 shows the arrival of fuel at spark plug during stratified operation. It presents a sequence of average images between 20 cycles. The operating conditions are 2000 rpm-BMEP 200 kPa-manifold pressure 80 kPa, with an end of injection timing of 70 CAD BTDC (or a beginning of

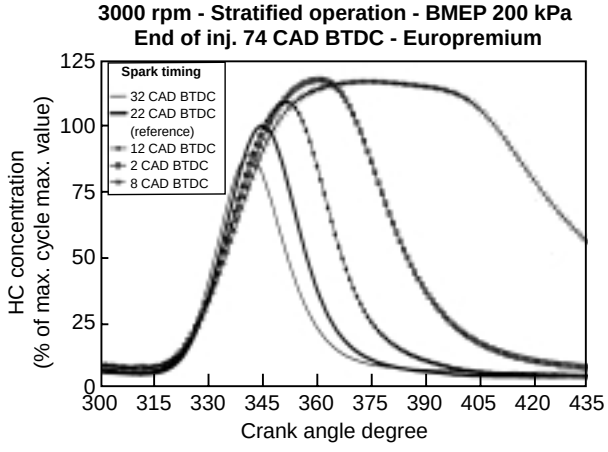

Figure 19

Variation in spark advance at 3000 rpm.

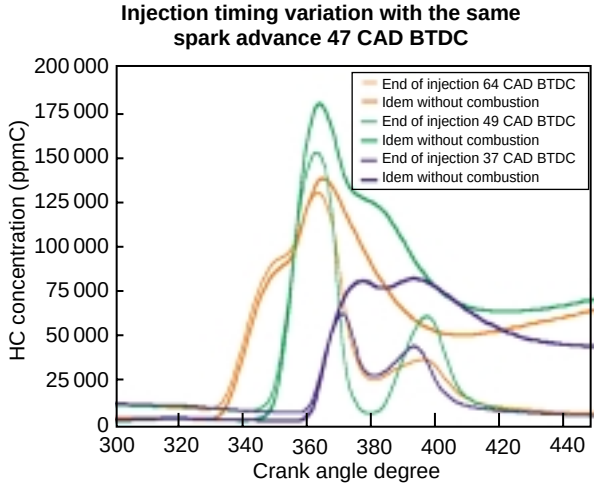

Figure 20

Influence of injection timing in stratified operation (spray guided) at 2000 rpm-IMEP 3.8 bar (1bar = 0.1 MPa).

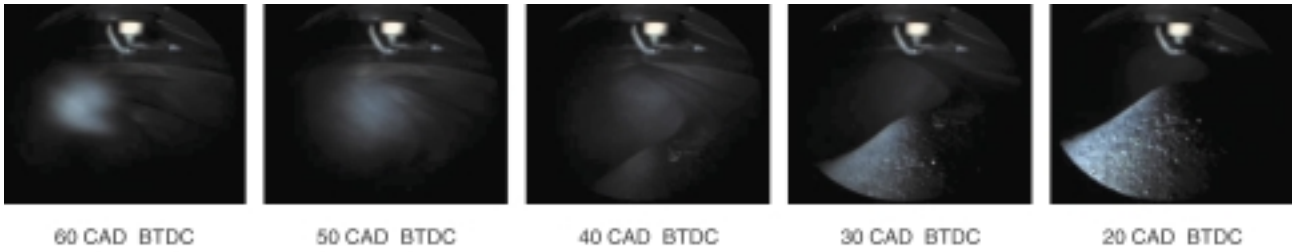

Figure 21

Visualization of injection in stratified mode - Average images between 20 cycles.

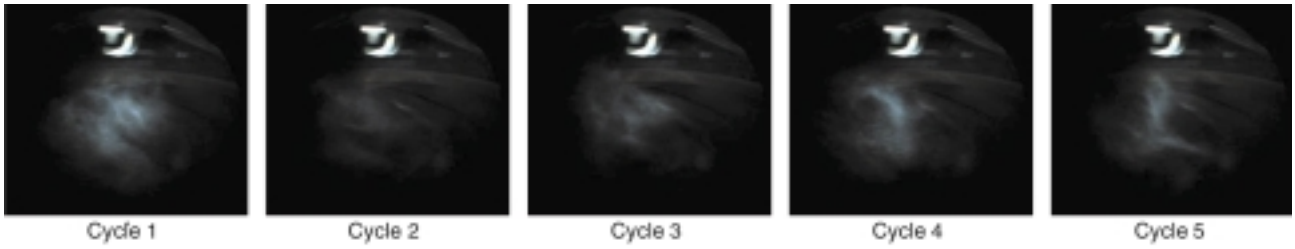

Figure 22

Visualization of injection in stratified mode - Individual cycles.

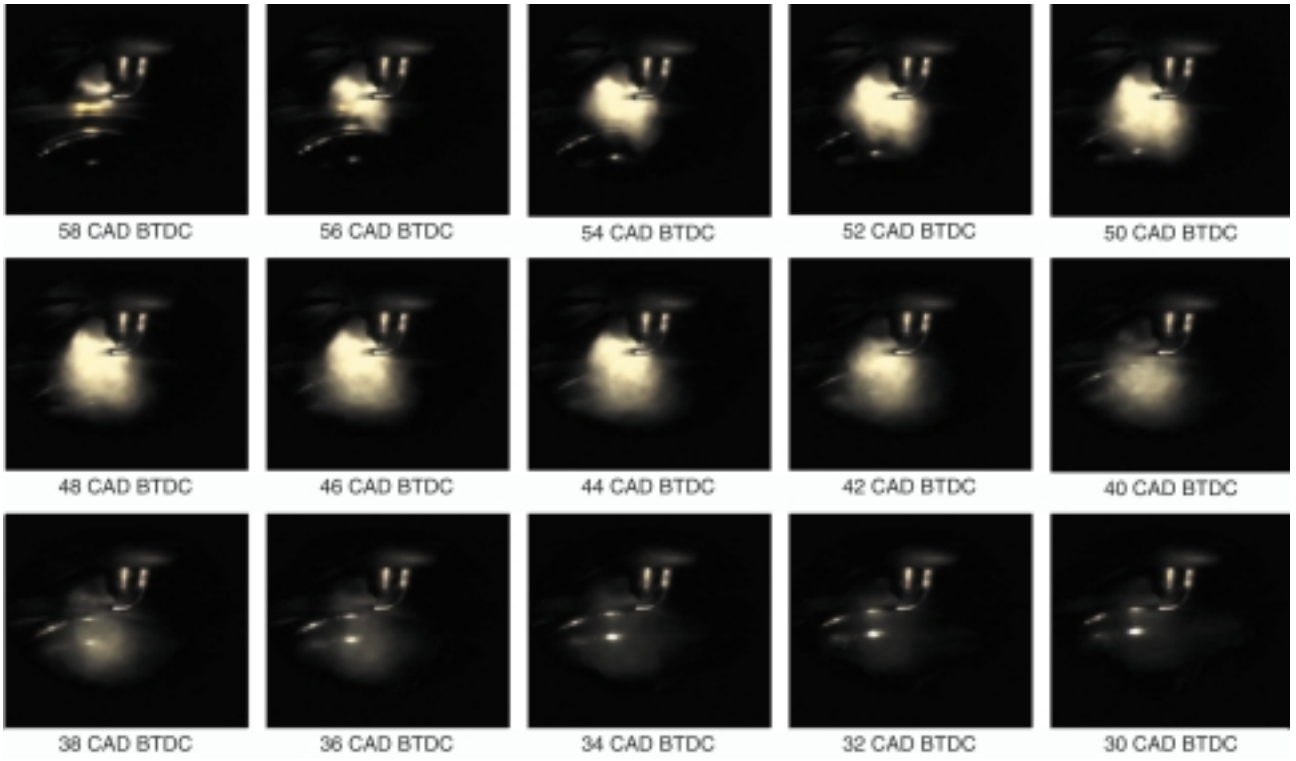

Figure 23

Visualization of injection in stratified mode - Average images between 5 cycles.

78 CAD BTDC). It confirms that one part of the fuel is directly positioned under the spark plug without impacting the piston, as it has been demonstrated by 3D calculation. Endoscopy also only makes it possible to see drops of a certain size. Above 40 CAD before top dead center, or 30 CAD after the end of injection, the drops are no longer visible due to vaporization of the fuel.

Note also that we found wide fluctuations from cycle to cycle in the position of the liquid fuel as shown by the sequence in Figure 22. These fluctuations are in relation with the fluctuations in fuel concentration at plug observed during the FID measurements.

Visualizations of Mixture Preparation on Spray Guided Engine

Figure 23 shows the arrival of fuel at spark plug during stratified operation (without ignition). It presents a sequence of average images between 5 cycles. The operating conditions are 2000 rpm-IMEP 380 kPa-manifold pressure 100 kPa, with an injection event between 65 and 49 CAD BTDC. Droplets are much more visible than with wall guided concept, which is coherent with the nearness of injector and spark plug. It can be noticed that first droplets arrive in the vicinity of spark plug 7 CAD after the beginning of injection, but that the spray is fully developed around 50 CAD BTDC. This spray remains stable up to 42 CAD BTDC (the 7 CAD between this angle and the end of injection are coherent with previous ones). Droplets disappear then progressively into vapor and are no more visible at 30 CAD BTDC.

Figure 24 shows the cycle to cycle fluctuations in the position of fuel droplets for an injection event between 65 and 49 CAD BTDC. Pictures have been taken at a visualization angle of 47 CAD BTDC corresponding to optimal beginning of spark event timing. These fluctuations are apparently lower than the one observed in the case of wall guided engine but correspond in fact to wide fluctuations in fuel concentration (as observed with FID measurements) because of the very high gradient of fuel concentration in the periphery of fuel spray.

Figure 25 shows the cycle-to-cycle fluctuations in the position of fuel droplets for an injection event between 53 and 37 CAD BTDC, *i.e.* later injection. Pictures have been taken at 35 CAD BTDC, *i.e.* 2 degrees after the end of injection, as for the previous injection timing. It can be noticed that spray penetration and cone angle are lower corresponding to higher air density and that swirls in the periphery of spray are more visible.

Figure 24

Stratified mode - End of injection 49 CAD BTDC - Individual cycles at 47 CAD BTDC.

Figure 25

Stratified mode - End of injection 37 CAD BTDC - Individual cycles at 35 CAD BTDC.

Figure 26

Stratified mode - End of injection 64 CAD BTDC - Individual cycles at 62 CAD BTDC.

Figure 26 shows the cycle-to-cycle fluctuations in the position of fuel droplets for an injection between 80 and 64 CAD BTDC. Pictures have been taken at 62 CAD BTDC, *i.e.* 2 degrees after the end of injection. Spray cone angle is much bigger as previously and swirls in the periphery of spray are less visible.

3.2 Modeling Part

3.2.1 Introduction

The aim of the work presented in this part was to use the experimental database available on the *Mitsubishi* GDI engine, to test and validate the 3D combustion models developed for KIVA-MB in a real engine configuration. We attempted to check the ability of the models to reproduce the progress of combustion for wide engine parameter variations. In particular, the experimental results for fuel concentration around spark plug obtained by the FID probes were used and compared with the same types of signal calculated by the KIVA-MB computer code.

3.2.2 Spray Modeling

Spray fitting certainly represents the most important part of this study. The main characteristics of the spray model used in a previous study [12] were retained: C_7H_{13} fuel, Rosin-Rammler's type distribution. Several parameters were modified to obtain a spray description closer to the constant pressure vessel visualizations, and attempted to reproduce the pre-jet identified in this case.

Figure 27 shows the results obtained by calculation in the constant-pressure vessel with KIVA-MB and the corresponding visualizations. At each moment, the two images to be compared are located one on the other. The width and penetration of the spray are similar during injection up to 3 ms. Note also that one of the important points in the modification of the spray is the addition of pre-injection. This serves to place fuel downstream from the main injection and thereby obtain a similar distribution at the end of injection (cf. images at 3 ms). This modification also has repercussions for injection in the chamber, as we shall show below.

3.2.3 Reference Point

As in the previous calculations [12], the spray can be broken down into two parts: the upper part places the fuel near the plug and the lower part directly impacts the piston. Figure 28 clearly shows the progress of these phases. It shows cross-sections of the chamber passing through the plane of symmetry, and in a perpendicular plane passing through the plug FID probe. The two FID probes are shown in the different sections. The cross gives the plug location.

When injection takes place in the engine, the successive sections show that the pre-injection phase, while accelerating the entertainment of the main injection, serves to place a first part of the fuel rapidly on the piston directly under the plug. Thus the rich zone around the plug first results from the upper part of the spray (sections at 50 CAD BTDC). In the next phase, the reverse tumble movement present in the chamber drives this part of the spray toward the plug, where it joins the fuel from pre-injection (sections 40 CAD BTDC to 20 CAD BTDC). In consequence, the air/fuel equivalent ratio obtained at the plug tends to increase as the fuel arrives, while mixing with the ambient medium. It can be observed that the conditions at the time of ignition are sufficient to initiate combustion satisfactorily.

3.2.4 Comparison with Signals from FID Probes

For comparison with the signal from the FID probe, a number of changes were added to the code to obtain a signal calculated by KIVA-MB, by trying in particular to take into account the zone of influence of the gases collected by the FID probe. In KIVA-MB we decided to calculate a mean of the HC content present in a sphere around certain points located downstream of each probe. This averaged signal was compared with the experimental results. From this comparison, we selected the point that gave the closest signal to the FID signal on the basic case.

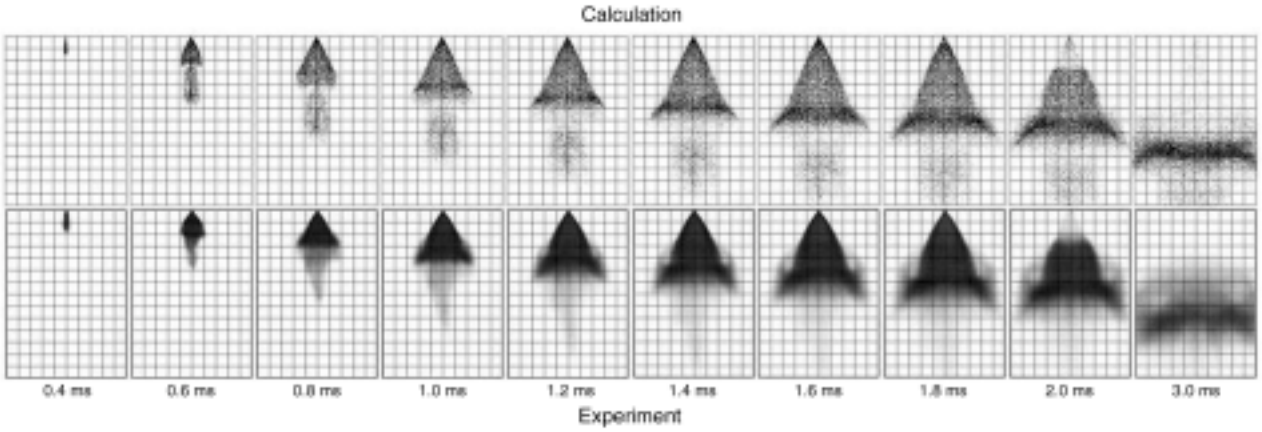

Figure 27

Spray structure - Comparison of visualizations and calculation by KIVA-MB.

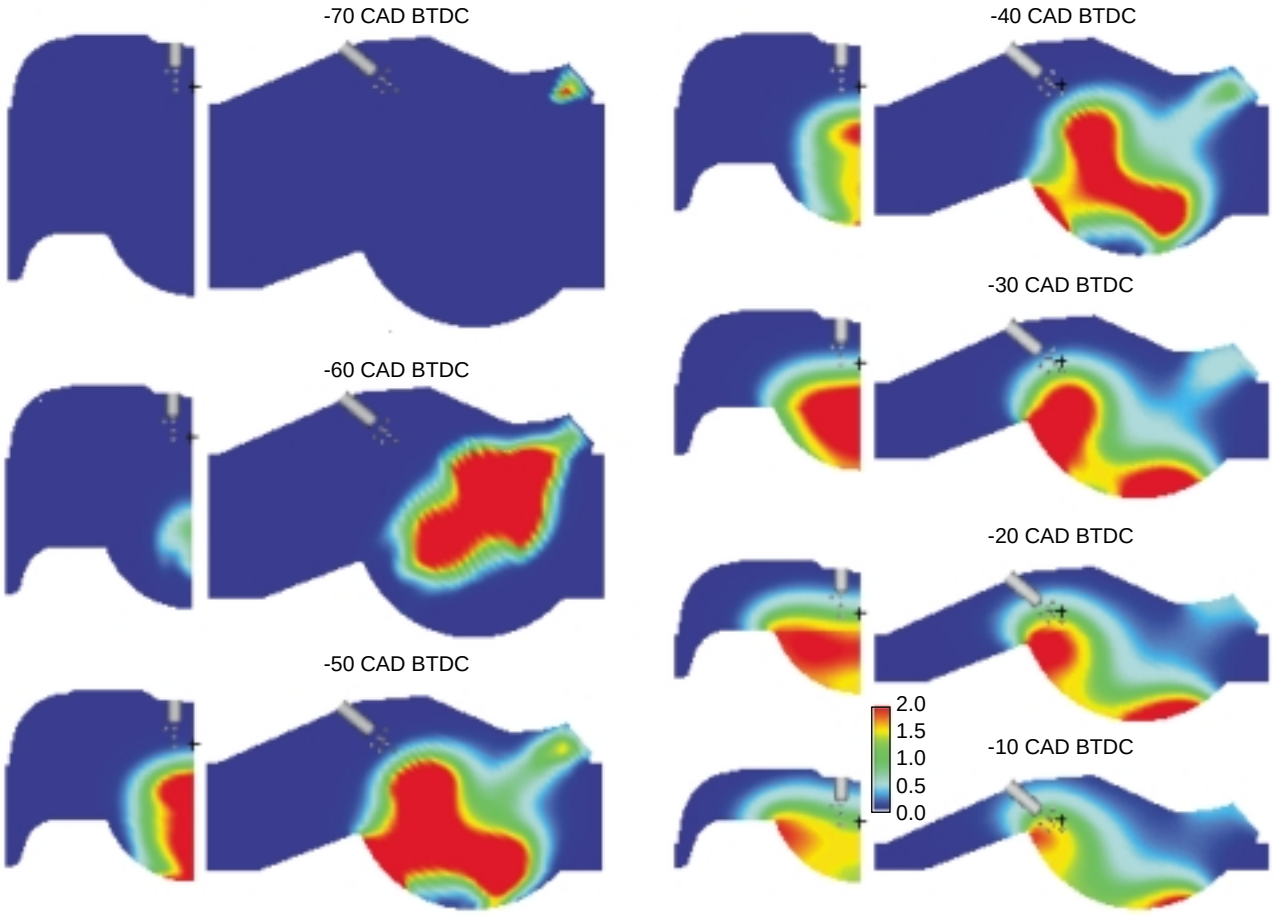

Figure 28

Variation of fuel/air equivalent ratio in the combustion chamber of *Mitsubishi* GDI engine.

The first part of Figure 29 gives the signal of these different points. Among them, the choice hence fell on the one placed at 3 mm downstream of each probe. The second part of Figure 29 shows that the comparison between the experimental signals and those given by KIVA-MB at 3 mm from the probe yields good results both on the cylinder head probe and on the plug probe. The graph also shows a curve indicating a long delay in spark advance, to be compared with the HC tracer calculated at the same point. The latter is a signal given by KIVA-MB without combustion. Looking at these two signals, it may be observed that the air/fuel equivalent ratio after stabilization (when combustion has not begun) is comparable between calculation and experiment.

It must be reminded here that the experimental curves of the FID signals cannot be used directly. They result from a calculation designed to take into account a transfer time from the chamber to the FID burner. Nevertheless, the response time of the probe is not corrected and explains that, in any cases, the rise of fuel concentration at spark plug occurs earlier in calculation than in experiment. In consequence, the following comparisons are more relative than absolute.

3.2.5 Spark and Injection Timing Variations

After this phase of software development on the reference case, variations were made in the engine parameters with the same tuning of spray parameters. We shall only discuss the main ones here: variation in injection advance (IT) or spark advance (SA). However, the speed, load and EGR ratios were also the subject of calculations and fairly satisfactory comparisons with experiment.

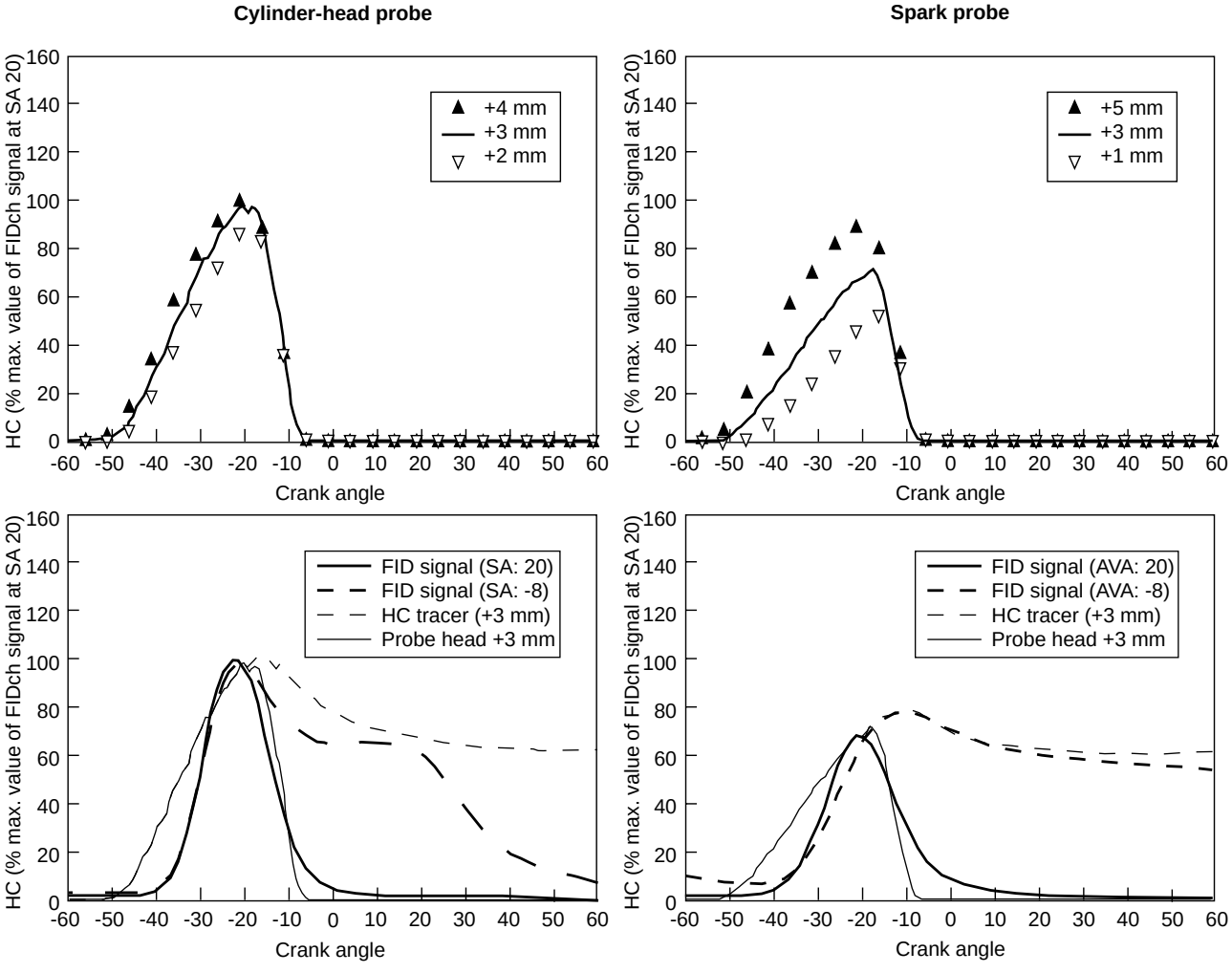

Figure 29

Fuel concentration at spark plug on the reference point: influence of calculation point location and comparison between calculation and experiment.

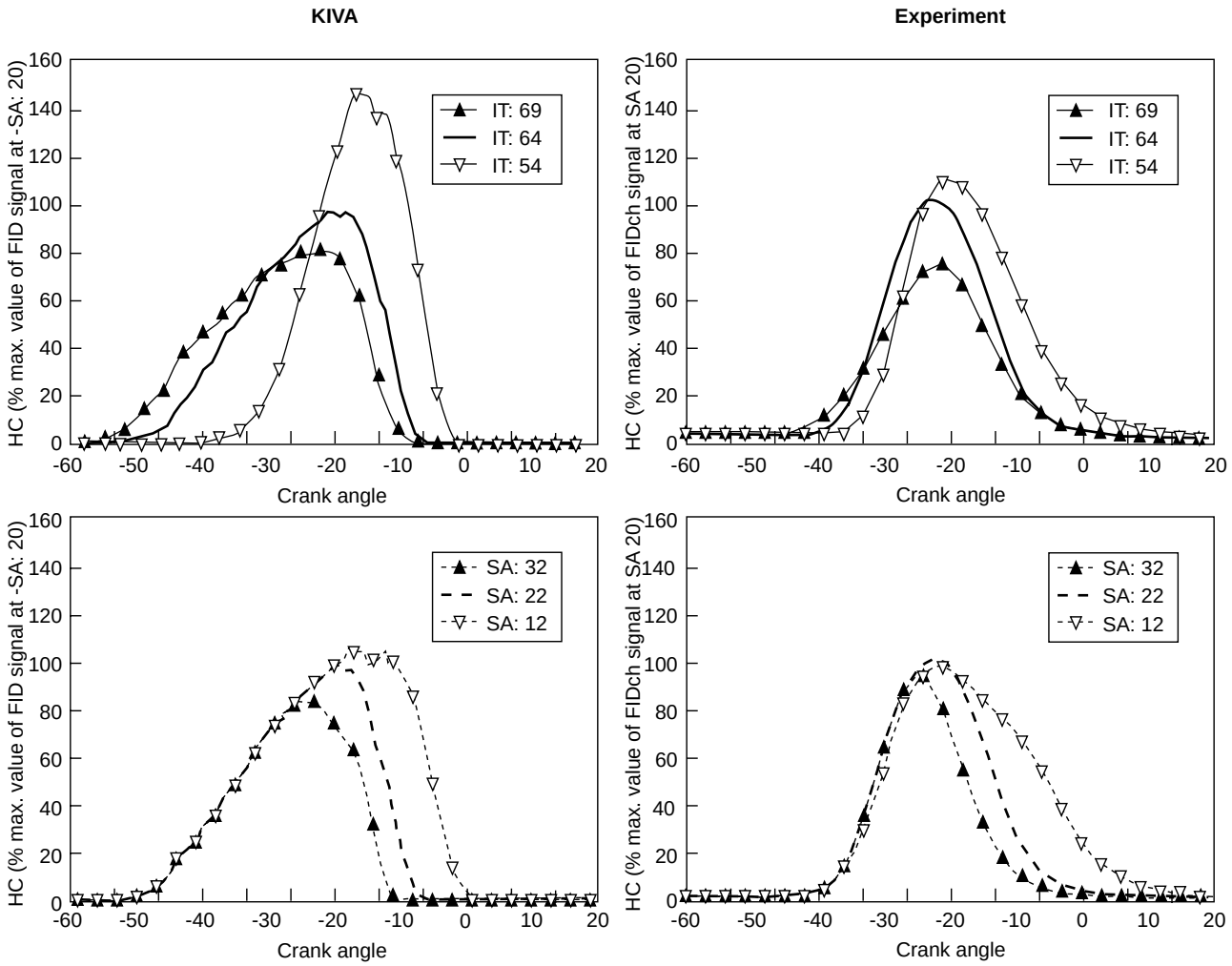

Figure 30

Air/fuel equivalent ratio at spark plug: calculation-experiment comparison during IT and SA variations.

Figure 30 shows injection timing variations for a spark advance of 22 CAD BTDC, and spark advances for an end injection advance of 64 CAD BTDC. The graphs in the first column give the calculated results that can be compared with the same experimental variations in the second column. By comparing the graphs placed side by side respectively, the same tendencies are found between the experimental results and those calculated by KIVA-MB with identical parameters. If the calculation overestimates the HC content for an IT of 54 CAD BTDC, what is probably due to a delay in the combustion beginning, the maximum values for the other cases are similar.

However, the overall results shown on Figure 30 revealed that the calculations fairly closely reproduce the air/fuel equivalent ratio variations around the plug.

4 STUDY OF COMBUSTION

4.1 Experimental Part

4.1.1 Combustion Visualizations on *Mitsubishi* Wall Guided GDI Engine

In the same way as for the mixture preparation, visualization by endoscopy proves to be a very useful tool for understanding the combustion phase. Cross-checking with cylinder pressure measurement reveals a good correlation and helps to clarify the cycle-to-cycle variations observed, as shown on Figure 31. For the visualization angle chosen (12 CAD BTDC), the earlier combustion is the more luminous one when we can not see any light for the latter. It can be noticed that for blue and red cycles, IMEP is the same, which

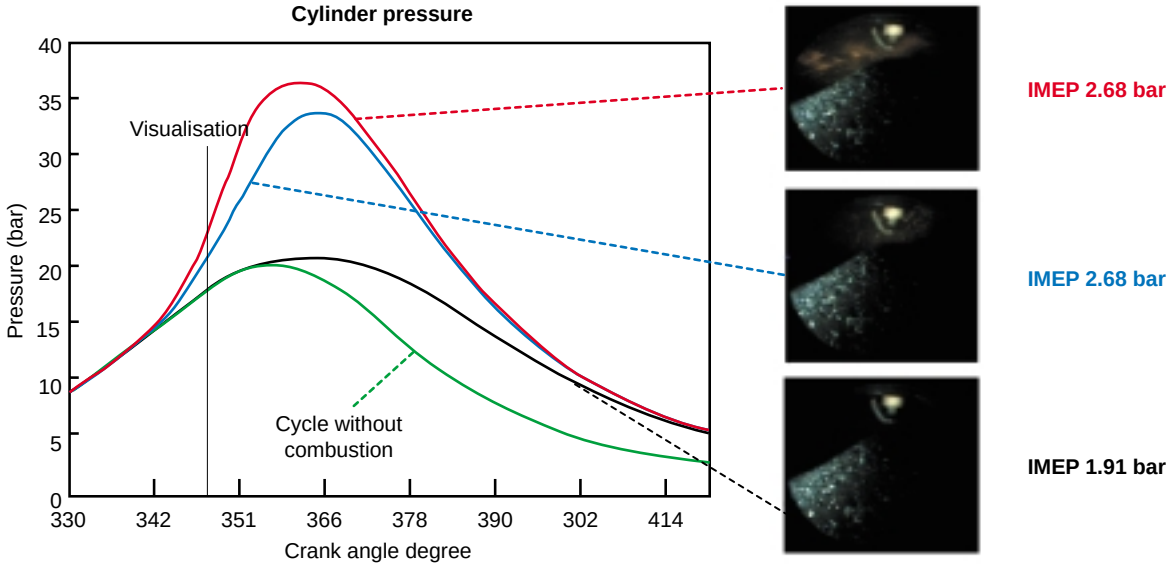

Figure 31

Cylinder pressure/combustion visualization correlation.

indicate that a very early combustion does not bring any increase in cycle efficiency despite higher cylinder pressure.

Endoscopy can also be used for a better understanding of the changes in combustion during parametric variations. To do this, we preferentially use a video film consisting of averaged images (from 20 images in general for considerations of memory size) from 50 CAD BTDC to 30 CAD ATDC with a constant step 20 CAD. Figure 32 shows an injection timing variation of +/-10 CAD around the reference value for the same spark timing.

This comparison shows that an injection advanced by 10 CAD (IT 80 CAD BTDC) results in a more homogeneous mixture which practically generates no combustion in "very rich" mode (hence smoke) but which burns at low air/fuel ratio producing a duller flame with sodium. This high air/fuel ratio combustion results in wide combustion instabilities and very little smoke. Note also that the fuel spray partially passes above the piston.

If injection is now delayed by 10 CAD (IT 60 CAD BTDC), the mixture is very stratified and very luminous combustion is observed. This luminous combustion (which is partially masked by the smoke deposit on the endoscope window) corresponds to diffusion flame, which generates smoke emissions. The analysis of the cycle-to-cycle IMEP shows that this combustion is very stable, because occurring in a rich zone. On the contrary, misfires are observed, because ignition takes place in the border of the zone containing fuel as shown by the calculation, and is very sensitive to cycle-to-cycle variations. The fuel spray in this case is confined by the piston. Smoke level is relatively high.

For the reference and later injections note also the presence of a luminous swirl at the end of combustion, corresponding to the combustion of the residual fuel stripped from the piston by the reverse tumble movement and the descent of the piston. This light corresponds to diffusion flame and shows that a great part of the smoke emissions comes from the late combustion of the part of fuel deposit on the piston which did not evaporate (which correlates with increasing smoke values when delaying the injection).

4.1.2 Combustion Visualizations on Spray Guided GDI Engine

Repeatability of Combustion Initiation

Figure 33 shows visualization of combustion initiation for 5 different cycles at the same angle on the set point 2000 rpm-IMEP 380kPa. Injection occurs between 65 and 49 CAD BTDC. Spark advance is 47 CAD BTDC and spark duration 2 ms (24 CAD). Visualizations have been performed 30 CAD BTDC.

Combustion initiation fluctuations are significant as well for flame shape as for flame position. It can be noticed that flame develops first in the direction of fuel droplets.

It must be reminded that this configuration allows only the visualization of diffusion flame because the device for seeding intake air with sodium borate (in order to see pre-mix type combustion) was not used on this engine, because of its high level of stratification.

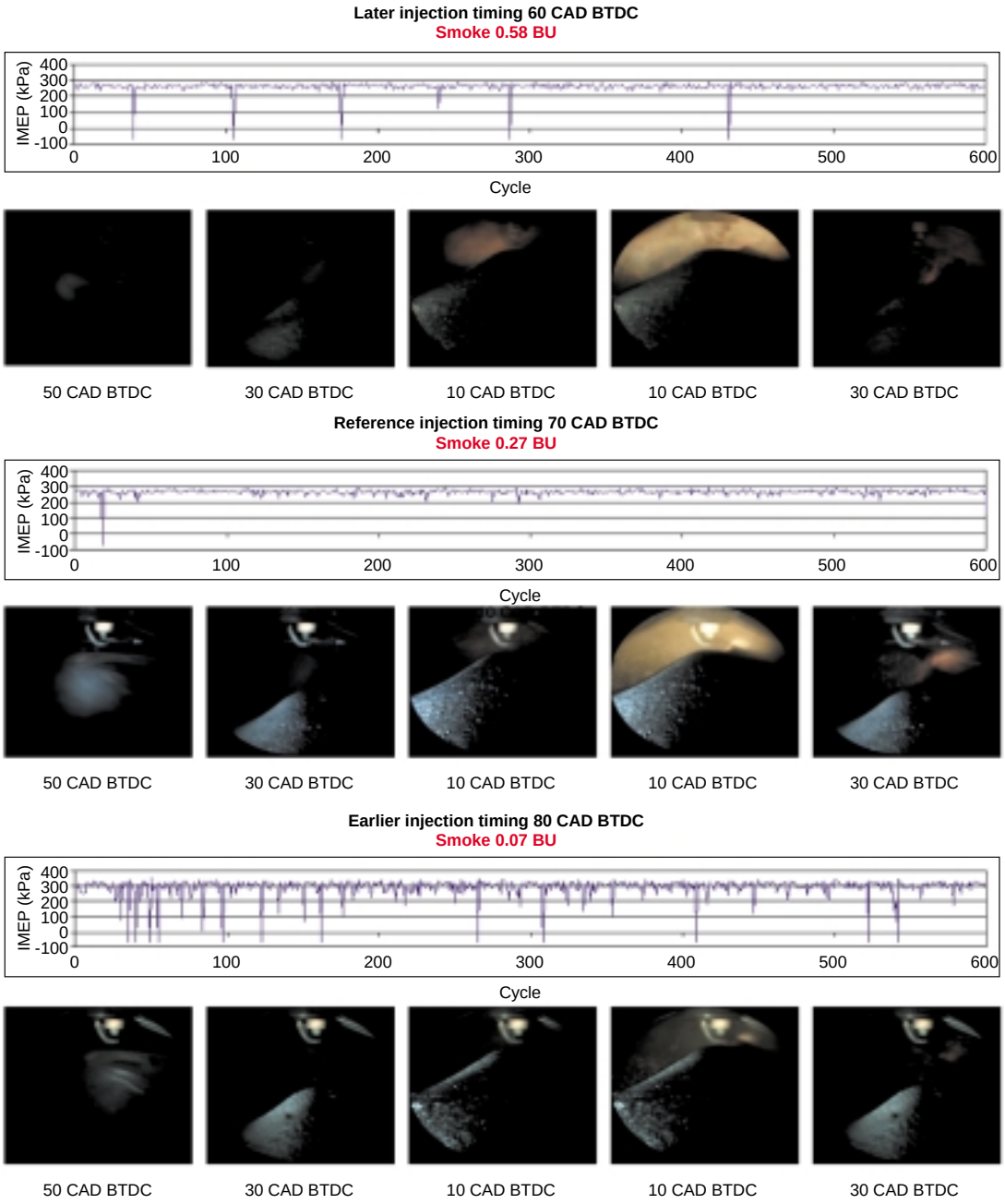

Figure 32

Influence of injection timing - Wall guided concept - 2000 rpm - BMEP 200 kPa - manifold pressure 80 kPa - SA 28 CAD BTDC.

Figure 33

Repeatability of combustion initiation - Spray guided concept - 2000 rpm-IMEP 380 kPa-manifold pressure 100 kPa - SA 47 CAD BTDC.

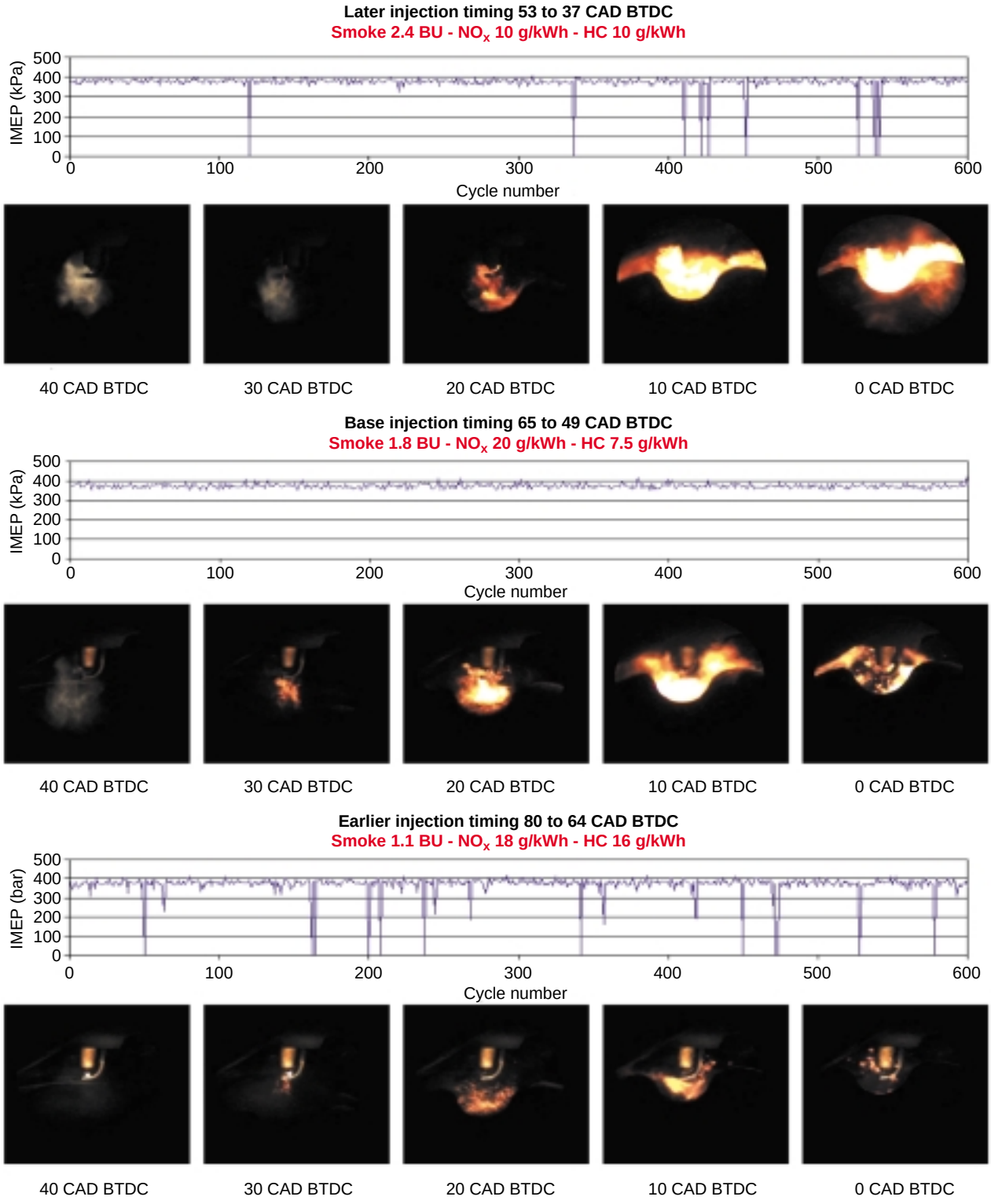

Figure 34

Influence of injection timing for spray guided concept - 2000 rpm-IMEP 380 kPa-manifold pressure 100 kPa - SA 47 CAD BTDC.

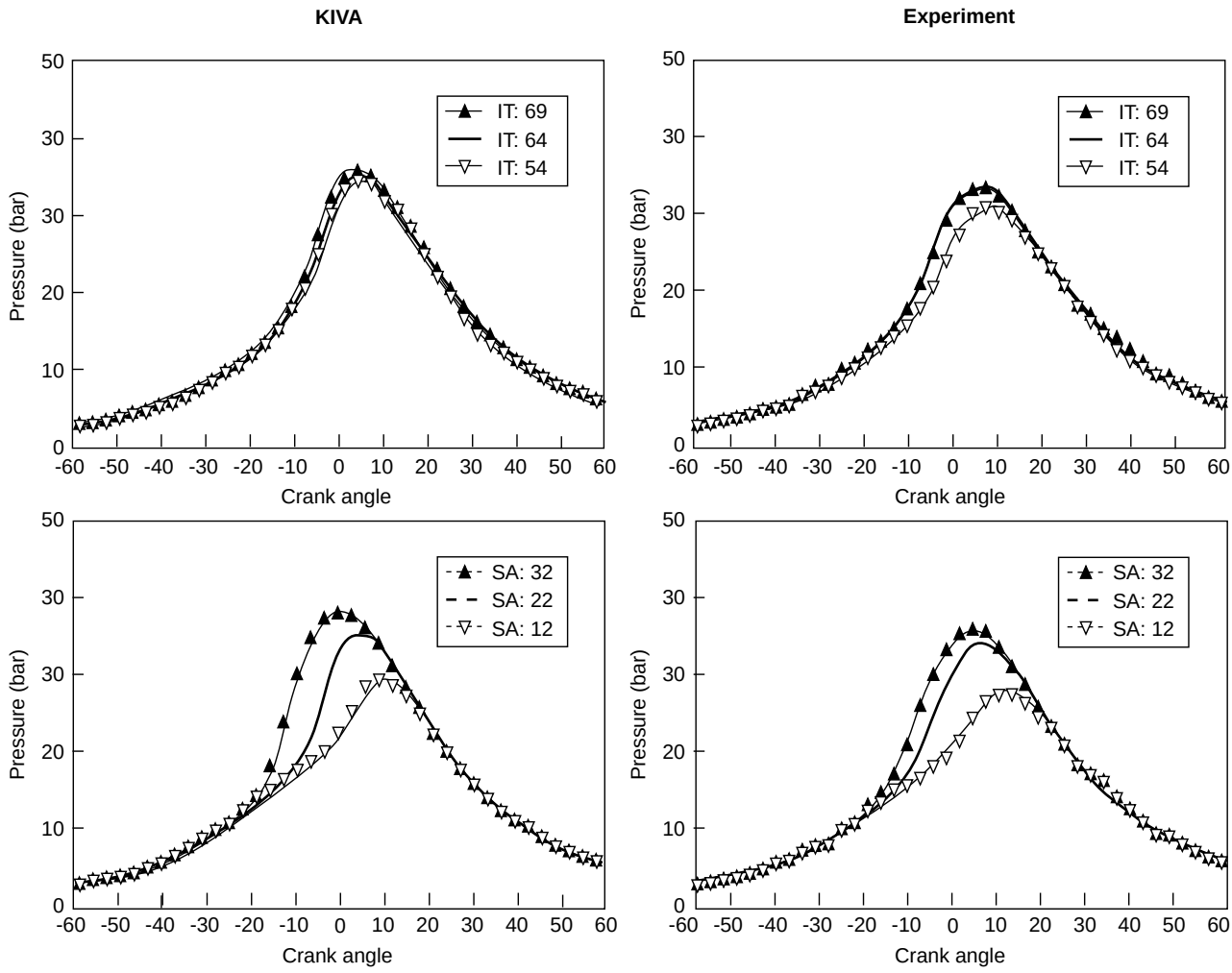

Figure 35

Cylinder pressure traces: comparison between calculations and experiments.

Influence of Injection Timing

Figure 34 presents the influence of injection timing on combustion event. All tests have been performed at 2000 rpm-IMEP 380 kPa with the same spark advance of 47 CAD BTDC and spark duration of 2 ms (24 CAD).

With basic injection timing, no misfiring occur and IMEP stability is rather good. Smoke level is much higher than for Mitsubishi engine.

With later injection, fuel droplets are still present during the first two pictures, *i.e.* during spark event. Ignition occurs later and combustion is much more luminous, corresponding to higher level of stratification. Misfiring cycle proportion is high but IMEP stability (apart from misfiring) is still good. Smoke level is high but NO_x emissions are divided by a factor 2.

With earlier injection, fuel droplets have already disappeared at 40 CAD BTDC. Ignition does not occur significantly before it does with basic injection timing. Flame is much less luminous, indicating a greater dilution of fuel into air and little fuel deposit on the piston bowl. Misfiring cycle proportion is also high and IMEP stability is bad. Smoke level is low, but HC emissions are high.

Note that in all cases the flame grows first in the direction of piston bowl, following the spray.

4.2 Combustion Calculation

Changes in the cylinder pressure according to the IT and SA are given on Figure 35 and compared with the experimental results.

Here also, it may be observed that the calculations closely reproduce the engine parametric variations, even if the maximum pressure is slightly overestimated in each case. Despite this, however, a good matching can be observed between the IMEP calculated from the KIVA-MB pressures and the IMEP obtained from the experimental pressure curves (see *Table 2*, where the "calculated IMEP" is obtained using the portions of the experimental pressure curves outside the 3D calculation range).

TABLE 2

IMEP calculations: comparison between calculations and experiments

Case	Calculated IMEP	Experimental IMEP
Reference	2.88	2.78
IT: 69	2.88	2.80
IT: 54	2.75	2.73
SA: 32	2.72	2.66
SA: 12	2.81	2.74

CONCLUSION

A methodology has been developed in order to characterize mixture preparation and combustion of gasoline direct injection engines even at a late stage of development. The 3D calculations and advanced experimental tools used in this study have proven to be in good agreement with this objective.

Endoscopic visualization in the cylinder offers a close understanding of the distribution of liquid fuel in the chamber as well as of the start of combustion. This was advantageously used to analyze the cyclic dispersion of combustion and correlates well with the IMEP measurements. The measurement of the air/fuel equivalent ratio at the spark plug by high-speed FID was the most important part of the experimental study. This measurement gives good results, even though the length of the FID probes means excessively long response time for use at high speed. It confirms the amplitude of the air/fuel ratio fluctuations at the spark plug. Despite these very large cycle-to-cycle variations, average measurements are reproducible and in good agreement with CFD calculations. Specific methodologies have been developed in order to qualify average behavior of mixture preparation for wall guided and spray guided concepts.

The results obtained by the 3D calculations on wall guided concept were similar to those obtained by experiment, as well as on mixture preparation and on the progress of combustion. A great work has been done on spray fitting to approach the visualizations in a constant pressure vessel as closely as possible. The comparison of the fuel concentration at the spark plug obtained by FID and KIVA-MB on the basic setting point as been also an important way for adjusting the spray model parameters. This final adjustment has been used successfully for other calculations, and good agreement with experiment is obtained during the variation of injection timing and spark advance.

Analysis of *Mitsubishi* 1.8 l GDI engine has been performed first with this approach. Practical conclusions of the analysis of this wall guided engine concept are the following.

- Very large cycle-to-cycle variations of air/fuel ratio at spark plug are observed in stratified mode. These variations are directly correlated to fluctuations of combustion starting, and then of IMEP.
- In stratified mode, one part of the fuel is carried-out directly from the injector to the spark plug without impinging the piston. This part of the fuel is directly concerned by ignition event.
- The behaviors of ignition and combustion in stratified mode are a function of injection timing. For injection earlier than optimum, ignition is reliable but combustion occurs with difficulty due to high air/fuel ratio. Conversely for injection later than optimum, some misfirings occur, but when not, combustion is fast.
- Nonevaporated fuel deposit in the piston bowl is related to smoke emissions.

Analysis of a spray guided direct injection engine concept has also been performed. Practical conclusions of the analysis of this wall guided engine concept are the following.

- Large cycles to cycle variations of fuel concentration around spark plug are observed in stratified mode. These variations are in relation with the very high stratification in the periphery of spray and with the little fuel spray moving from one cycle to another due to injector repeatability and aerodynamic motion.
- In the case of early injection fuel spray cone angle is larger. Combustion stability is bad. Misfirings occur and could be in relation with too rich mixture at spark plug.
- In the case of late injection, the spray cone angle shrinks due to higher air density. Ignition occurs in the swirl of spray and begins later. High stratification and fuel deposit in piston bowl generates luminous combustion, high smoke level and low NO_x emissions. Misfirings occur but, when not, combustion stability is rather good.

ACKNOWLEDGEMENTS

The authors would like to express thanks to the *Groupement Scientifique Moteur* (*Renault SA*, *Peugeot Citroën SA* and *IFP*) and *French Ministry of Industry* for supporting this work.

The authors will also to thank personally MM. P. Voisard and N. Tourteaux from *Peugeot Citroën SA*, as well as MM. C. Voisin, E. Vidal, P. Gastaldi and R. Bonetto from *Renault SA* for the very constructive discussions we had all along this program, as well as MM. E. Chevé, F. Guerbet, H. Ravelojaona and M. Zolver from *IFP* for their important contributions to this study.

REFERENCES

1 Zhao, F, Lai, M.C. and Harrington, D.L. (1997) A Review of Mixture Preparation and Combustion Control Strategies for Spark Ignited Direct Injection Gasoline Engines. *SAE Paper 970627*.

2 Zhao, F., Lai, M.C. and Harrington, D.L. (1999) Automotive Spark-Ignited Direct-Injection Gasoline Engines. *Progress in Energy and Combustion Science*, **25**.

3 Kume, T., Iwamoto, Y., Murakami, M., Akishino, K. and Ando, H. (1996) Combustion Control Technologies for Direct Injection SI Engine. *SAE Paper 960600*.

4 Iwamoto, Y., Noma, K., Nakayama, O. and Ando, H. (1997) Development of Gasoline Direct Injection Engine. *SAE Paper 970541*.

5 Ando, H., Noma, K., Lida, K., Nakayama, O. and Yamauchi, T. (1997) Mitsubishi GDI Engine Strategies to Meet the European Requirements. *Engine and Environment Conference 97*, Graz, Austria.

6 Ando, H. (1998) Mixture Preparation in Gasoline Direct Injection Engines. *FISITA Paper F98T050*.

7 Crawford, J.G. and Wallace, J.S. (1996) Validation Tests for a Fast Response Flame Ionization Detector for In-Cylinder Sampling Near the Spark Plug. *SAE Paper 961201*.

8 Kakuhou, A., Urushihara, T., Itoh, T. and Takagi, Y. (1999) Characteristics of Mixture Formation in a Direct Injection SI Engine with Optimezed in-cylinder Swirl Air Motion. *SAE Paper 1999-01-0505*.

9 Summer, T. and Collings, N. (1995) Modelling the Transit Time of a Fast Response Flame Ionization Detector During In-Cylinder Sampling. *SAE Paper 950160*.

10 Collings, N., Wai, K.Cheng and Galliot, F. (1989) On the Time Delay in Continuous In-Cylinder Sampling From IC Engine. *SAE Paper 890579*.

11 Peckham, M. and Collings, N. (1994) FID Capillary Flow Theory. *Seminar Proceedings at the Institution of Mechanical Engineers*, London.

12 Duclos, J.M. and Zolver, M. (1998) 3D Modeling of Intake, Injection and Combustion in a DI-SI-Engine under Homogeneous and Stratified Operating Conditions. *Comodia 98*.

Final manuscript received in November 2002